Unclassified/Unlimited
SECURITY CLASSIFICATION OF THIS PAGE (When Data Entered)

REPORT DOCUMENTATION PAGE

READ INSTRUCTIONS BEFORE COMPLETING FORM

1. REPORT NUMBER: No. 43
2. GOVT ACCESSION NO.:
3. RECIPIENT'S CATALOG NUMBER:

4. TITLE (and Subtitle): Micro-Undulator FEL Technology

5. TYPE OF REPORT & PERIOD COVERED: Technical Report 10/01/84 - 09/30/85

6. PERFORMING ORG. REPORT NUMBER:

AUTHOR(s): Luis Elias and Gerald Ramian

8. CONTRACT OR GRANT NUMBER(s): N00014-80-C-0308

PERFORMING ORGANIZATION NAME AND ADDRESS:
University of California
Quantum Institute
Santa Barbara, CA 93106

10. PROGRAM ELEMENT, PROJECT, TASK AREA & WORK UNIT NUMBERS: 61153N; RR011-07-06; NR603-001

CONTROLLING OFFICE NAME AND ADDRESS:
ONR
1030 E. Green St.
Pasadena, CA 91106

12. REPORT DATE: 1985

13. NUMBER OF PAGES:

14. MONITORING AGENCY NAME & ADDRESS(if different from Controlling Office):

15. SECURITY CLASS. (of this report): Unclassified/Unlimited

15a. DECLASSIFICATION/DOWNGRADING SCHEDULE:

16. DISTRIBUTION STATEMENT (of this Report)

Approved for public release; distribution.

17. DISTRIBUTION STATEMENT (of the abstract entered in Block 20, if different from Report)

18. SUPPLEMENTARY NOTES

Proceedings of the International Conference of Lasers '84, 1985

19. KEY WORDS (Continue on reverse side if necessary and identify by block number)

Micro-Undulator, FEL

20. ABSTRACT (Continue on reverse side if necessary and identify by block number)

A novel technique for overcoming lower size limitations in the fabrication permanent magnet undulators is described. An analysis of the properties of such millimeter period undulators is presented and some possible low-voltage FELs employing them are discussed.

90 05 17 068

DD FORM JAN 73 1473

Unclassified/Unlimited

MICRO-UNDULATOR FEL TECHNOLOGY

L. Elias, G. Ramian

Lasers '84 Publication QIFEL043/85

MICRO-UNDULATOR FEL TECHNOLOGY

L.ELIAS AND G.RAMIAN

QUANTUM INSTITUTE
UNIVERSITY OF CALIFORNIA
SANTA BARBARA,CA. 93106

ABSTRACT

A novel technique for overcoming lower size limitations in the fabrication of permanent magnet undulators is described. An analysis of the properties of such millimeter period undulators is presented and some possible low-voltage FELs employing them are discussed.

INTRODUCTION

Electrostatic accelerators have been demonstrated[1] to be cheap, compact, reliable sources of stable, low energy-spread, low emittance electron beams for FELs. Additionally the incorporation of beam recirculation provides high overall efficiency. These advantages are, however, offset by the long wavelengths imposed by relatively low voltages.

$$\lambda = \frac{\lambda_o}{2\gamma^2}$$

λ_o = undulator period
γ = relativistic mass ratio

For example, the UCSB FEL currently operates at a minimum wavelength of 380μ at 3 MV.

Shorter wavelengths can of course be achieved by building accelerators of higher voltage. A 25 MV accelerator is presently operating at Oak Ridge National Laboratory and with further development[2], terminal voltages as high as 40 MV might be attained. Although competitive with other types of accelerators, these are still large costly machines requiring extensive laboratory facilities including radiation shielding. A more attractive approach to shorter wavelengths would involve the use of smaller period undulators with the lower voltage machines. Experience with the UCSB undulator[3], however, suggests that construction with individual magnets in a Halbach, or any other, configuration of significantly shorter period than our present 3.6 CM, would involve prohibitive difficulties not only in dealing with mechanical complexity on a miniature scale, but also in dealing with material strength limitations. Our present Samarium-cobalt magnets, for example, require stainless steel sheathing to avoid spontaneous fracture caused by the the large torques and forces induced by adjacent magnets as assembly proceeds.

With these problems in mind, alternative approaches to the generation of undulator fields that at least avoid tiny magnets were sought. An initial suggestion[4] was made to record an undulator field pattern on thin strips of Chromium-Cobalt in a process similar to tape recording. Theoretically, an adequate undulator field could be generated in this manner but so far, only small fields have been observed. While work will continue on this approach, Samarium-Cobalt, in the form of large blocks, appears to provide a more immediately practical approach.

DESCRIPTION

Figure 1b illustrates the micro-undulator configuration. In contrast with the Halbach configuration (Fig. 1A), it consists simply of grooves ground in blocks of Samarium-Cobalt. Typically, a 3 MM period would require 1.5 MM x 1.5 MM grooves. The grinding of such grooves is routine, but other limitations apply. According to manufacturers we have contacted, one of the most difficult steps in the manufacture of Samarium-Cobalt involves pressing and sintering at high pressure while an intense magnetic field maintains grain orientation. Current production machinery imposes an approximate size limit of 2 x 2 x 1/2 inch.

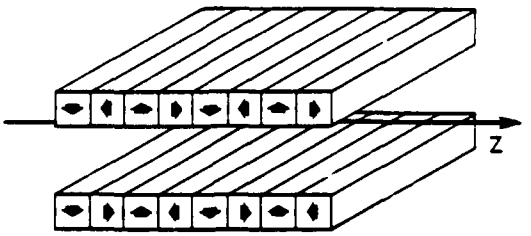

Fig. 1A **HALBACH CONFIGURATION**

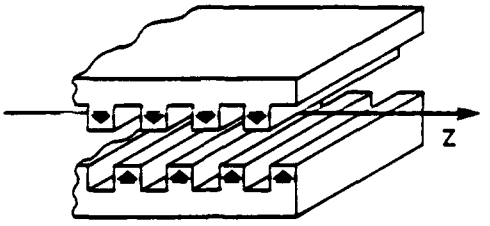

Fig. 1B **MICRO-WIGGLER**

MAGNETIC FIELDS

Numerical analysis of the magnetic fields generated by the micro-undulator configuration was performed by relaxing a two dimensional mesh with a finite difference approximation to Poisson's equation. The properties of Hitachi H90B material, including its intrinsic demagnetization, were used for convenience although better materials are now available. The field plots are shown in Fig. 2

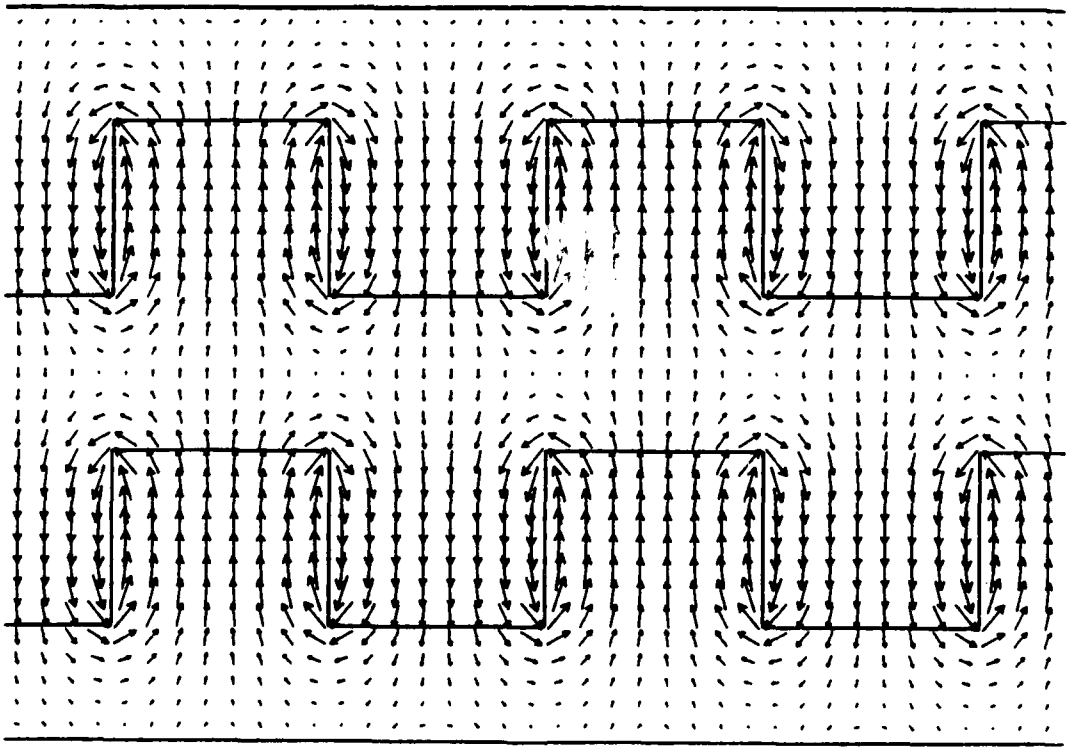

Fig. 2 Micro-Undulator Field Plot

Inherent in the modeling of a three dimensional problem in two dimensions, is the assumption that the model is a constant cross-section extending to infinity in the third dimension. In this case, consequently, no flux return path is provided and the solid portion of the magnetic material above and below the grooves contributes nothing to the undulator fields which are generated entirely by the material between grooves. In effect, a demagnetization field H is generated exactly equal and opposite the magnetic moment M, resulting in zero B field . An actual undulator, with finite dimensions, would have a flux return path resulting in the transverse fields shown in Fig. 3. Similar fields would be present at the ends. The most difficult problem thus created, is the presence of a strong quadrupole field in the area of the electron beam as shown in Fig. 4. For the example shown, with a gap to width ratio of 1:20, a k_Q value of 810 G/CM results. k_Q is expected to vary inversely with the cube of width, so a sufficiently large transverse dimension combined with horizontally oriented compensation magnets as shown in Fig. 5 should correct this effect. The same transverse corrector magnets could make the end fields axially symmetric, turning them effectively into focussing solenoids.

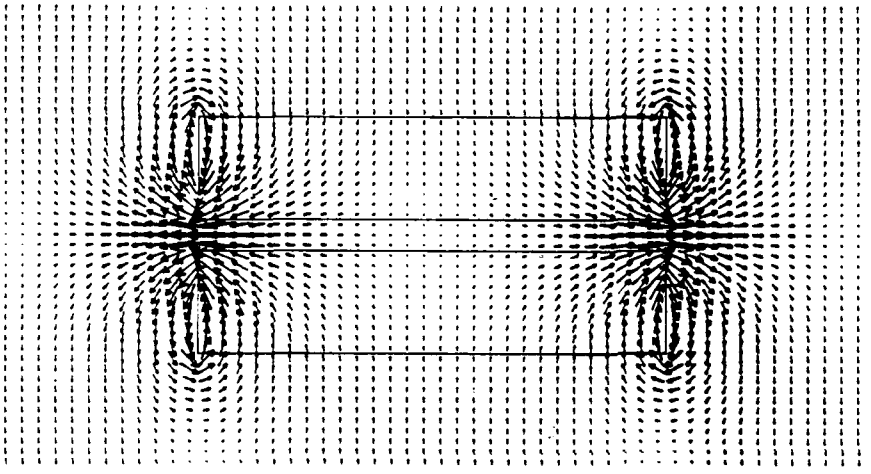

Fig. 3 Transverse Field Plot

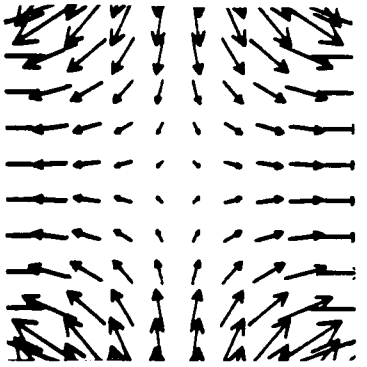

Fig. 4 Quadrupole Field in Central Region

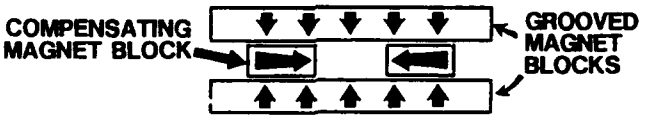

Fig. 5 Quadrupole Field Compensation

As explained earlier, only material between grooves contributes to the undulator field and since, as verified by the numerical simulation, the nearly ideal properties of Samarium-Cobalt result in less than a 5% change in magnetic moment over the range of demagnetizing forces involved, a simple analytic model of the micro-undulator is possible. MKS units are assumed. Separation of variables in Laplace's equation

$$\nabla^2\phi = 0 \qquad , \ \phi = \text{magnetic scalar potential}$$

leads to a Sturm-Liouville boundary value problem in two dimensions, with a general Fourier series solution

$$\phi = \sum (A_n \sin nkx + B_n \cos nkx)(C_n \sinh nky + D_n \cosh nky)$$

$$\text{,where } k = \frac{2\pi}{\lambda_o}$$

The boundary conditions leading to the definition of coefficients A_n, B_n, C_n, and D_n are shown in Fig. 6. Note that in this analysis, x is the longitudinal dimension.

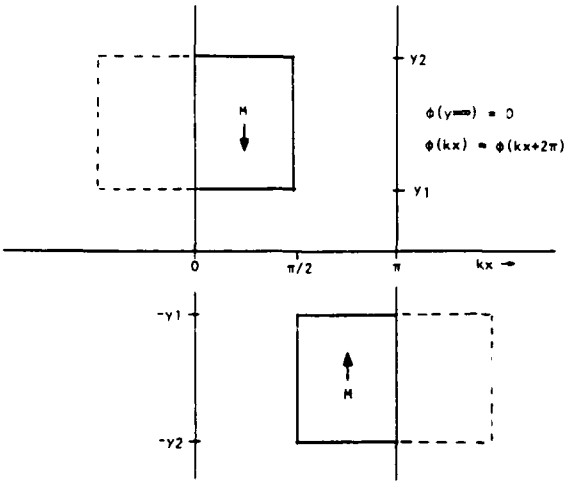

Fig. 6 Two Dimmensional Boundary Value Problem

The condition that $\phi = 0$ at $y = \infty$ requires that $C_n = -D_n$. The magnet position is chosen to make the solution a cosine series in x ($B_n = 0$) so ϕ, after redefining A_n as A_nC_n, is expressed as

$$\phi = \sum (A_n \cos nkx)(\sinh nky - \cosh nky) \qquad (1)$$

The magnet boundary conditions require that B-perpendicular and H-tangential be continuous across a boundary, leading to a discontinuity in $\frac{d\phi}{dy}$ equal to $\frac{M}{2}$ at the boundaries at y1,y2,-y1, and -y2 in Fig. 6. A_n can now be determined by equating the derivative of (1) with respect to y

$$\frac{d\phi}{dy} = \sum nk(A_n \cos nkx)(\cosh nky - \sinh nky) \qquad (2)$$

term by term with the magnet boundary discontinuity expressed as the Fourier series of a rectangular function

$$\frac{d\phi}{dy} = \sum \frac{M}{n\pi}(\cos nkx) \qquad , n = 1,3,5,...$$

at each of the four y boundaries and then summing. Replacing cosh - sinh terms with exponentials, the sum, with respect to an arbitrary position y, is

$$e^{-nk(y1-y)} + e^{-nk(y1+y)} - e^{-nk(y2-y)} - e^{-nk(y2+y)}$$

which after expanding then factoring out a cosh term becomes

$$2\cosh nky\ (e^{-nky1} - e^{-nky2})$$

After replacing M with B_r/μ_o, and since in air, $B_y = \mu_o \frac{d\phi}{dy}$, the final expression for B_y is

$$B_y = \frac{2B_r}{\pi} \sum (\cos nkx)(\cosh nky)(e^{-nky1} - e^{-nky2}) \qquad (4)$$

$$, -y1 < y < y1$$

It is unnecessary to do anything further with ϕ as its only purpose was to guaranty that (4) satisfies Laplace's equation. Fig. 7A is a plot of By as a function of gap to period ratio and Fig. 7B is a plot of By and it's harmonics as a function of y.

A test of the micro-undulator concept was performed with magnets already on hand. The magnet dimensions (.8 x.8 x10 CM) resulted in a 1.8 CM period. Fig. 8 is a plot of the measured fields. No attempt was made to match magnets so field irregularities are expected. The average peak field on axis is in agreement with both the numerical and analytical models.

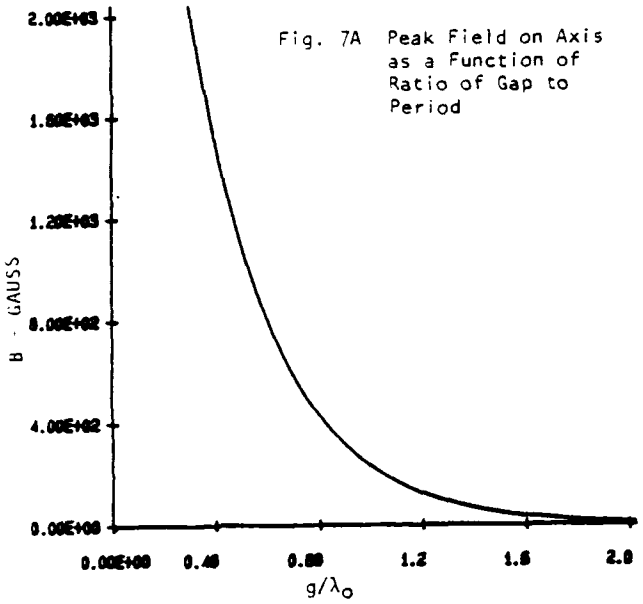

Fig. 7A Peak Field on Axis as a Function of Ratio of Gap to Period

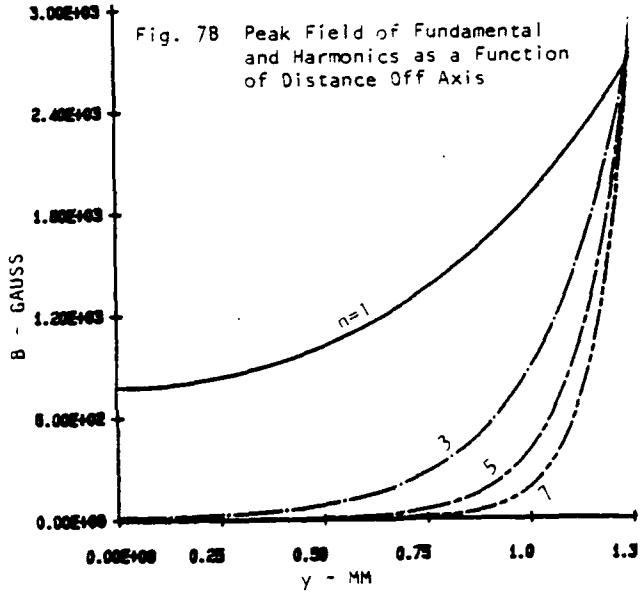

Fig. 7B Peak Field of Fundamental and Harmonics as a Function of Distance Off Axis

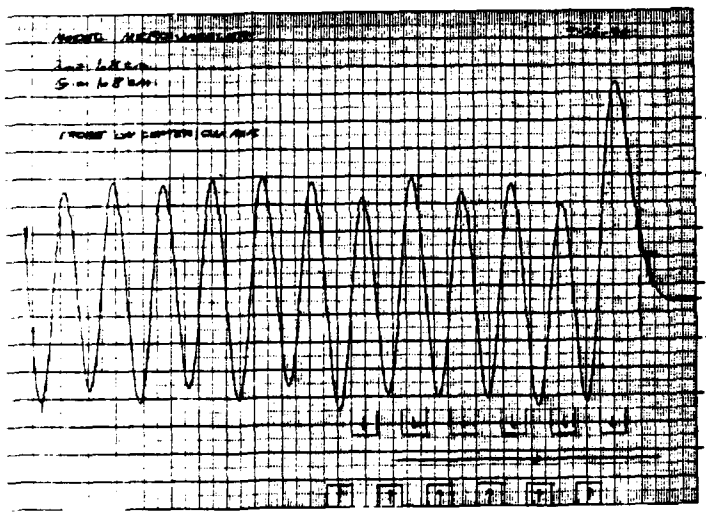

Fig. 8 Measured Fields of Large Magnets in a Micro-Undulator Configuration

	UCSB FEL	MW 1	MW 2	MW 3
V	3.0 MV	1.0 MV	1.5 MV	3.0 MV
γ	6.87	2.95	3.93	6.87
λ	380 μ	312 μ	158 μ	49 μ
λ_o	3.6 CM	5.3 MM	4.8 MM	4.6 MM
g	3.8 CM	3.0 MM	2.2 MM	1.3 MM
Bo	413 G	895 G	1255 G	2180 G
Am	2.4 CM^2	.014 CM^2	.01 CM^2	.006 CM^2
Ib	1.25 A	1.25 A	1.25 A	1.25 A
L	5.76 M	.5 M	.5 M	.5M
N	160	94	104	109
Ps	11.7 KW	6.6 KW	9.0 KW	17.2 KW
εb	7.5 *	5.0 *	3.75 *	2.2 *
Yb	3.0 MM	.74 MM	.54 MM	.33 MM

TABLE 1

FEL Parameters

* π MM-MR

FELs

Although micro-undulators hold promise at any wavelength or electron beam energy, our present interests are in the FIR wavelengths. Three possible designs have been considered. Energies of 1.0, 1.5, and 3.0 MEV were chosen corresponding to standard NEC horizontal accelerators. An undulator length of .5 M was arbitrarily chosen and a tradeoff with other parameters is certainly possible. Table 1 shows parameters of these FELs as well as the parameters of the recently demonstrated UCSB FEL. Maximum utilization of existent technology was considered important and to that end, elements of the present UCSB FEL design such as the electron gun and the hybrid waveguide resonator[5] were incorporated. Parameters have been chosen primarily to scale small-signal gain to to that of the present FEL.

$$G \propto \lambda_o B^2 I L^3 \gamma^{-3} A_m^{-1} \qquad (3)$$

In these examples, beam size in the narrow vertical dimension of the waveguide is confined by the betatron focussing force of the undulator. Fig. 9 is a plot of equilibrium radius as a function of emittance for a 1.5 MEV beam with a 530 G peak undulator field. At 0 emittance, space charge force alone results in a .14 MM radius while for an expected emittance of 3.75 MM-MR, the radius is .54 MM. An undulator gap of 4 times this radius was provided for beam clearance. In an actual design, a more conservative value might be appropriate. Fig. 10 is a plot of gap as a function of period derived by folding peak field as a function of gap to period ratio along with the mode area filling factor into the gain proportionality relation (5), for 1.5 MEV. For example, a gap of 2.2 MM requires a period of 4.8 MM, yielding 158 μ radiation.

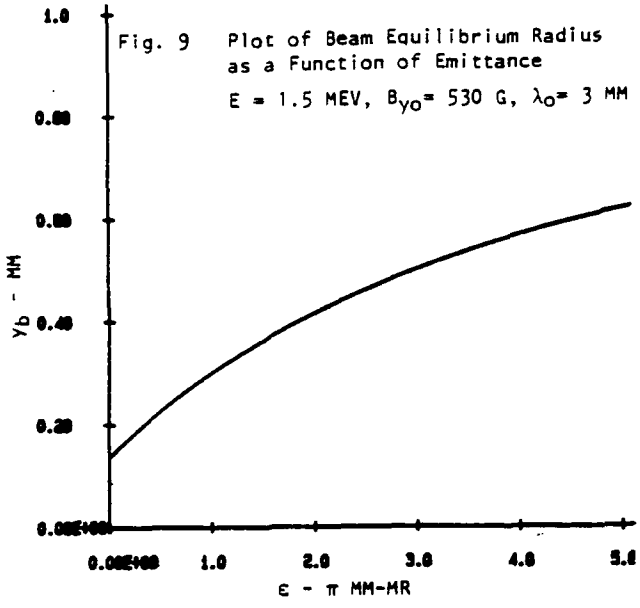

Fig. 9 Plot of Beam Equilibrium Radius as a Function of Emittance

E = 1.5 MEV, B_{yo}= 530 G, λ_o= 3 MM

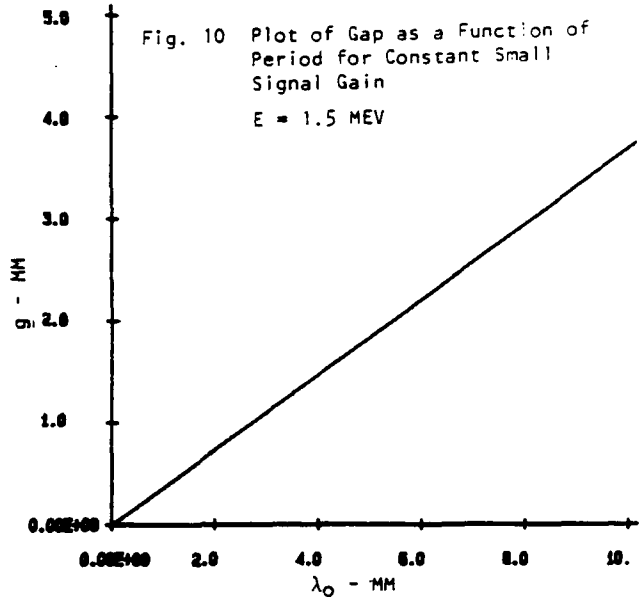

Fig. 10 Plot of Gap as a Function of Period for Constant Small Signal Gain

E = 1.5 MEV

Fig. 11 is an illustration of a 1MV Fel. Several innovations make possible the relatively compact size. First, the small size of the micro-undulator permits installation within the accelerator terminal. This requires a positive terminal potential which allows about twice the field gradient of negative terminal machines, permitting use of a smaller tank.
The short direct electron beam path means less degradation of beam quality from transport over long distances through many beam optical components. This also means less beam loss and less x-radiation. In fact, it is NEC's current practice to shield the 1.0 and 1.5 MV machines by wrapping the tanks with lead sheeting. This advantage is underscored by the present UCSB machine which requires a building with 2 foot thick concrete walls for shielding. Also, the electronic components associated with the gun, collector, corona triode, and other things would be outside the tank, significantly enhancing reliability. It might even be possible to completely eliminate electronic components from the terminal by using permanent magnet beam optic components inside. Of course, beam diagnostics within the terminal remains a serious problem.

Fig. 12A and 12B are photographs of NEC's 1.0 and 1.5 MV accelerators. The 1.0 MV machine is shown wrapped with lead shielding. The 1.5 MV machine is shown in a laboratory setting similar to what we envision as a complete FEL installation.

CONCLUSION

The micro-undulator concept offers exciting possibilities in a wide range of applications both in terms of reduced FEL size and shorter wavelength operation. Compact FELs operating in the FIR wavelengths based on current FEL and electrostatic accelerator technology appear to be viable concepts.

1 MEV FEL

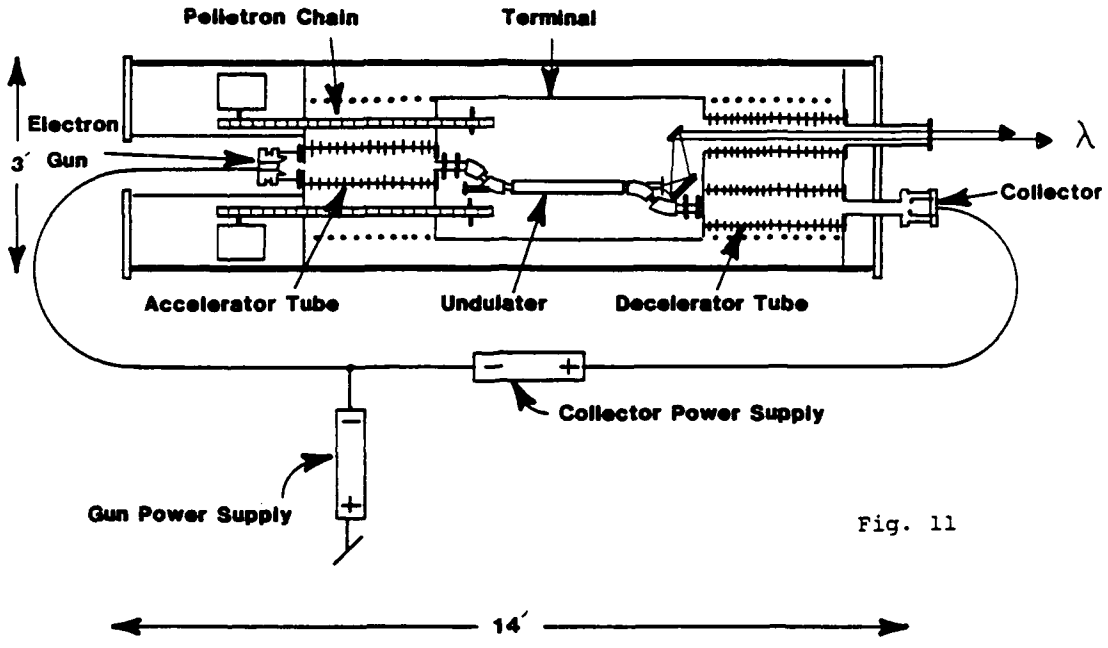

Fig. 11

Fig. 12A

NEC 1 MEV Accelerator

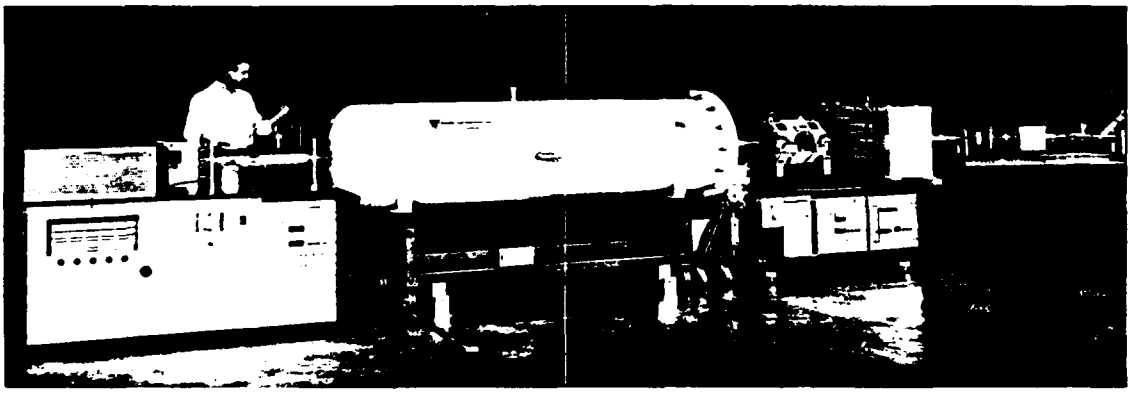

Fig. 12 B NEC 1.5 MEV Accelerator

REFERENCES

1. "Results of the UCSB FEL Electron Beam Recirculation Experiment," Elias,L., Ramian,G., Proceedings of the International Conference on Lasers '82, Society for Optical and Quantum Electronics, STS Press, McLean, VA., 1982, p154

2. Personal communication with R. Herb of National Electrostatics Corp., Middleton, Wisconsin

3. "Properties of the UCSB FEL Wiggler," Elias,L., Hu,J., Ramian,G., Free Electron Generators of Coherent Radiation, SPIE Vol. 453, 1983, p160

4. Personal communication with W. Yen of University of Wisconsin and "Magnetic Structure for a Microundulator," White,R.M., Applied Physics Letters, V44, No.2, Jan,1985

5. "Cylindrical Gaussian-Hermite Modes in Rectangular Waveguide Resonators," Elias,L., Gallardo,J., Applied Physics B, Springer-Verlag, 1983, Vol 31, p229

---

* Research supported under ONR contract N00014-80-C-0308